



Infection-elicited microbiota promotes host adaptation to nutrient restriction

Mirian Krystel De Siqueira^{a,1,2}, Vinicius Andrade-Oliveira^{b,c,2,3} , Apollo Stacy^{b,c,2,4,5}, João Pedro Tôrres Guimarães^a, Ricardo Wesley Alberca-Custodio^a , Angela Castoldi^a, Jaqueline Marques Santos^a, Marcela Davoli-Ferreira^a, Luísa Menezes-Silva^a, Walter Miguel Turato^d, Seong-Ji Han^{b,c,6}, Arielle Glatman Zaretsky^{b,c,7}, Timothy Wesley Hand^{b,8}, Niels Olsen Saraiva Câmara^a, Momtchilo Russo^a, Sonia Jancar^a, Denise Moraes da Fonseca^{a,2,5}, and Yasmine Belkaid^{b,c,2,5}

Contributed by Yasmine Belkaid; received October 21, 2022; accepted December 14, 2022; reviewed by Wendy S. Garrett and Manuela Raffatellu

The microbiota performs multiple functions vital to host fitness, including defense against pathogens and adaptation to dietary changes. Yet, how environmental challenges shape microbiota resilience to nutrient fluctuation remains largely unexplored. Here, we show that transient gut infection can optimize host metabolism toward the usage of carbohydrates. Following acute infection and clearance of the pathogen, mice gained more weight as a result of white adipose tissue expansion. Concomitantly, previously infected mice exhibited enhanced carbohydrate (glucose) disposal and insulin sensitivity. This metabolic remodeling depended on alterations to the gut microbiota, with infection-elicited *Betaproteobacteria* being sufficient to enhance host carbohydrate metabolism. Further, infection-induced metabolic alteration protected mice against stunting in the context of limited nutrient availability. Together, these results propose that alterations to the microbiota imposed by acute infection may enhance host fitness and survival in the face of nutrient restriction, a phenomenon that may be adaptive in settings where both infection burden and food precarity are prevalent.

host metabolism | white adipose tissue | carbohydrate | malnutrition | *Yersinia*

The survival of living organisms relies on their ability to adapt to environmental fluctuations and challenges. In this regard, the symbiotic alliance between the host and its microbiota is essential for optimal host physiology and fitness in the face of environmental stressors (1–3). A vast array of biodiverse ecosystems and complex interaction networks, the gut microbiota intimately shapes human physiology through its regulation of host immunity and metabolism (4). A principal trait of the gut microbiota is its versatility in extracting energy from the biochemically diverse components (carbohydrates, protein, and fat) of the omnivorous human diet (5). This versatility extends from the microbiota's remarkable capacity to adapt both functionally and rapidly to host dietary changes (6). Because of this, one of the greatest environmental drivers of microbiota diversity and metabolic output is host diet, not only its components but also fluctuations in its availability. For example, the malnutrition widespread in under-resourced settings can compromise the gut microbiota's development and diversity (7). In contrast, a high-fat Western diet can dramatically remodel the microbiota (6) and promote metabolic syndrome, a cluster of conditions including high blood glucose, triglycerides, and body fat [white adipose tissue (WAT)] that increases risk for diabetes and other health conditions (8).

While host diet plays an outsized role in regulating the microbiota, the microbiota can in turn regulate host usage and storage of diet-derived energy. Illustrating this, germfree mice devoid of microbiota are protected against diet-induced obesity (9), accumulating less WAT than conventional mice (10). Furthermore, host metabolism can be regulated, either favorably or detrimentally, by defined taxa within the microbiota. For example, the mucus-degrading bacterium *Akkermansia muciniphila* protects against obesity and diabetes (11), while the deltaproteobacterium *Bilophila wadsworthia*, which expands in response to fat-induced bile acids (12), can aggravate metabolic syndrome (13).

Besides host diet, environmental stressors such as infection and antibiotics can also impact the microbiota. Indeed, in industrialized countries, changes in the infectious landscape combined with nutritional alterations and the overuse of antibiotics are strongly associated with a decline in gut microbiota diversity and the recent, concomitant rise in various inflammatory and metabolic diseases (14). Accordingly, some degree of pathogen exposure may benefit the host by helping to maintain a diverse gut microbiota and disease resistance (15). Further, exposure to pathogens may in fact be necessary for the microbiota to optimally develop and maintain host fitness. Supporting this idea, the microbiota of wild mice, which encounter more pathogens than laboratory mice, limits influenza infection and colon cancer, while also protecting against obesity and metabolic syndrome (16, 17). Similarly, self-limited gut infection can induce changes

Significance

The long-term impacts of infection on the microbiota and its regulation of host physiology are poorly understood. Here, we report that long-term alterations to the gut microbiota following a single, acute episode of bacterial or protozoan gut infection can remodel host metabolism to preferentially and more efficiently consume carbohydrates. This infection-triggered metabolic remodeling ultimately results in white adipose tissue expansion and host weight gain. Furthermore, in the context of low limited nutrient availability, infection-triggered carbohydrate metabolism benefits host fitness by preventing host stunting. Our study suggests a new perspective in which infection (pathogen-induced stress) can be co-opted as a cue to prime host adaptation to nutritional stress.

²M.K.D.S., V.A.-O., A.S., D.M.d.F., and Y.B. contributed equally to this work.

³Present Address: Center for Natural and Human Sciences, Federal University of ABC, Santo André SP 09210-580, Brazil.

⁴Present Address: Department of Cardiovascular and Metabolic Sciences, Lerner Research Institute, Cleveland Clinic, Cleveland, OH 44195.

⁵To whom correspondence may be addressed. Email: stacya2@ccf.org, denisefonseca@usp.br, or ybelkaid@niaid.nih.gov.

⁶Present Address: Jill Roberts Institute for Research in Inflammatory Bowel Disease, Joan and Sanford I. Weill Department of Medicine, Department of Microbiology and Immunology, Weill Cornell Medicine, Cornell University, New York, NY 10021.

⁷Present Address: Regeneron Pharmaceuticals, Tarrytown, NY 10591.

⁸Present Address: R.K. Mellon Institute for Pediatric Research, Pediatrics Department, Infectious Disease Section, University of Pittsburgh Medical Center Children's Hospital of Pittsburgh, University of Pittsburgh, Pittsburgh, PA 15224.

This article contains supporting information online at <https://www.pnas.org/lookup/suppl/doi:10.1073/pnas.2214484120/-DCSupplemental>.

Published January 18, 2023.

to the microbiota that enhance its resistance to subsequent pathogen encounters (18). In contrast, dysregulated host metabolism can disrupt or alter the microbiota's resistance to pathogens (19, 20), but to date, whether infection can in turn impact the microbiota's regulation of host metabolism warrants further exploration.

Here, we show that prior gut infection, long after clearance of the pathogen, can promote WAT expansion and host weight gain, while at the same time optimizing host metabolism for carbohydrates. This shift toward carbohydrates, characterized by enhanced glucose disposal and insulin sensitivity, occurs in a microbiota-dependent manner, with infection-elicited *Betaproteobacteria* being sufficient to enhance carbohydrate usage. Furthermore, infection-optimized host carbohydrate metabolism can prevent stunting in the context of nutrient restriction, a phenomenon that we speculate may sustain host fitness in settings where infection and food precarity often co-occur.

Results

Prior Gut Infection can Remodel WAT Physiology. To explore the impact of infection on host metabolism, we took advantage of the

Yersinia pseudotuberculosis (*Yptb*) model of transient gut infection (21). *Yptb* is a food-borne bacterial pathogen that causes transient weight loss in mice (Fig. 1A) before being cleared from the gut and peripheral tissues within 4 weeks (wk) post-infection (21).

At >15 wk post-infection, previously *Yptb*-infected (post-*Yptb*) mice began to gain more weight than naïve control mice (Fig. 1A). This increase was not associated with increased food intake (*SI Appendix*, Fig. S1A). X-ray imaging revealed significant expansion of peripheral body fat (Fig. 1B), with the weight of three major WAT depots—mesenteric, perigonadal, and subcutaneous—significantly increased in post-*Yptb* mice compared to naïve mice (Fig. 1C). In line with this observation, post-*Yptb* mice produced higher circulating levels of adiponectin, a hormone secreted primarily by WAT (Fig. 1D).

WAT expansion can be driven by an increase in the size (hypertrophy) of adipocytes and/or proliferation (hyperplasia) of progenitors (22). In all three depots, there was a greater frequency of smaller adipocytes in post-*Yptb* mice than naïve mice, ruling out a role for hypertrophy (Fig. 1E and *SI Appendix*, Fig. S1B and C). We next assessed WAT adipocyte progenitors for expression of the proliferation marker Ki-67 (gating strategy in *SI Appendix*, Fig. S1D). We chose to perform this analysis at a relatively early time point (4 wk

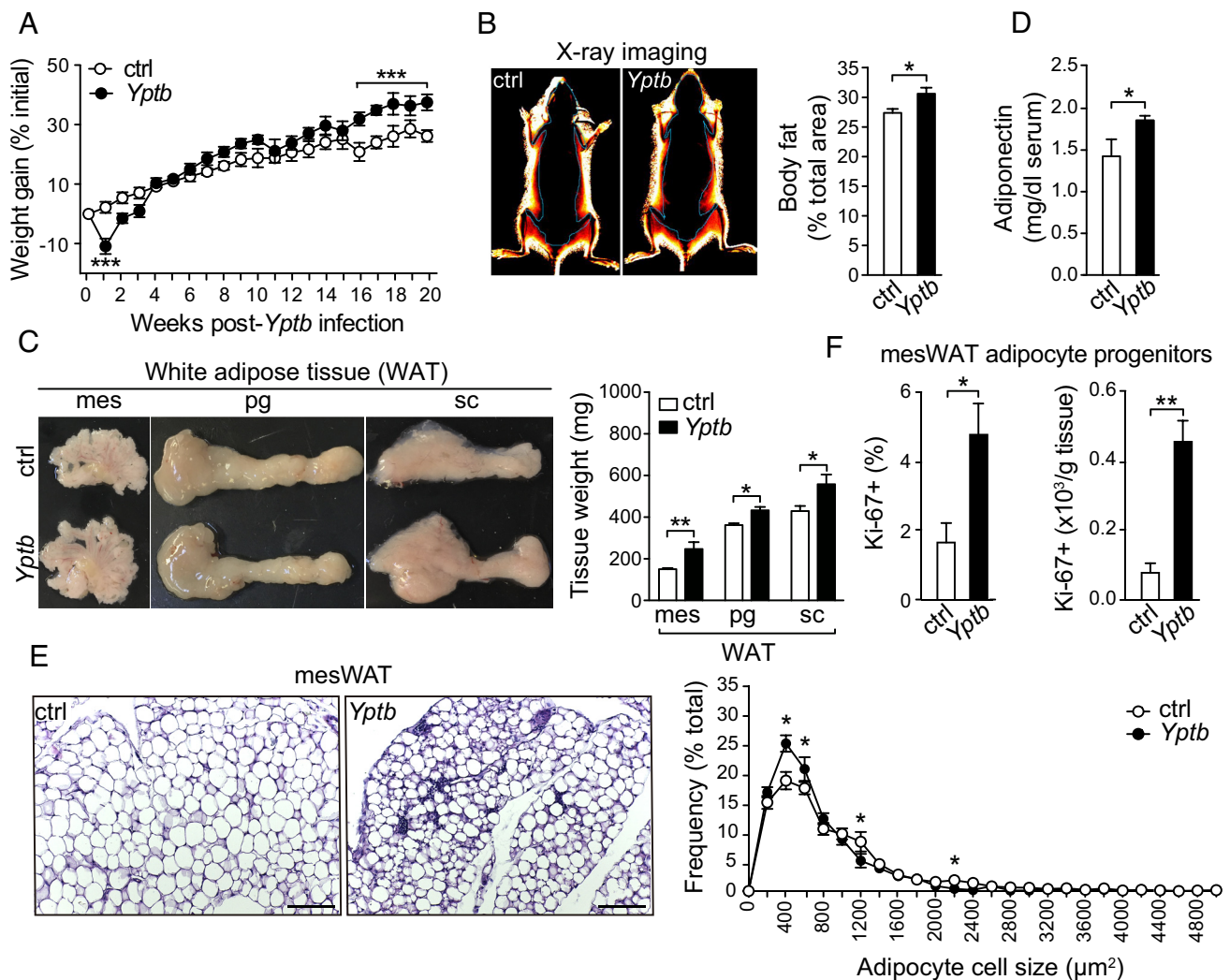


Fig. 1. Prior gut infection can remodel WAT physiology. (A–F) Analyses were performed at (B–E) >15 or (F) 4 wk post-*Y. pseudotuberculosis* (*Yptb*) infection. Naïve mice were used as a control (ctrl). (A) Weight gain (% initial) over time. (B) Representative X-ray images (Left) and quantification (Right) of peripheral body fat (% total area). (C) Representative images (Left) and quantified weights (Right) of WAT depots (mes, mesenteric; pg, perigonadal; sc, subcutaneous). (D) Adiponectin levels in the serum of fasting mice. (E) Representative images of H&E-stained mesWAT tissue sections (Left) and quantification of adipocyte cell size distribution (Right). Each x-axis tick mark corresponds to a bin size of 200 μm². (Scale bar: 100 μm.) (F) Frequency (Left) and number (Right) of proliferating (Ki-67+) mesWAT adipocyte progenitors. Data represent mean ± SEM (n ≥ 4 mice per group). *P < 0.05; **P < 0.01; ***P < 0.001 by two-tailed Student's *t* test. Data are representative of at least two experiments.

post-infection), reasoning that heightened proliferation would precede the expansion of WAT first observed at >15 wk post-infection. Adipocyte progenitors in the mesenteric and perigonadal but not the subcutaneous WAT of post-*Yptb* mice were more proliferative (as assessed by Ki-67+ cell frequency and number) than those of naïve mice, supporting a role for increased adipocyte hyperplasia (Fig. 1*F* and *SI Appendix, Fig. S1 E and F*). Thus, prior gut infection can induce physiological remodeling (associated with expansion and increased cell proliferation) of WAT and increased weight gain long-term after pathogen clearance.

Prior Gut Infection can Improve Host Metabolism. To assess the physiological consequences of post-infection WAT expansion, we first assessed circulating triglyceride levels. Post-*Yptb* mice had lower levels of triglycerides than naïve mice, suggesting that triglycerides were preferentially stored in WAT (Fig. 2*A*). In line with this, post-*Yptb* mice also had lower circulating levels of free glycerol, indicating that following infection, mice also reduce triglyceride breakdown into free glycerol and fatty acids (Fig. 2*B*). Thus, prior infection may increase host energy storage in the form of WAT triglycerides.

We next performed two common assessments of glucose metabolism: the glucose and insulin tolerance tests (GTT and ITT,

respectively). In the GTT, blood glucose levels are monitored at regular intervals after administering glucose, while in the ITT, blood glucose levels are monitored at regular intervals after administering insulin (23). Post-*Yptb* mice disposed glucose more efficiently, according to the GTT (Fig. 2*C*), and responded to insulin more sensitively, according to the ITT (Fig. 2*D*). Thus, despite expansion of WAT, prior gut infection can actually improve rather than negatively impact host metabolic parameters (triglyceride levels, glucose disposal, and insulin sensitivity) for the long-term.

Locally Constrained Gut Infection can Improve Host Metabolism. Previously, we showed that infection with *Yptb* permanently damages gut-associated lymphatic structures (21). Because these structures are crucial for the transport of lipids (21), we assessed if post-infection “scarring” of lymphatics could contribute to host metabolic alterations. To this end, we employed an attenuated form of *Yptb*, $\Delta yopM$, that lacks the virulence factor YopM (24) and as such is rapidly cleared from the gut and does not cause lymphatic scarring (24). Similarly to what we observed with *Yptb*, mice previously infected with $\Delta yopM$ also exhibited increased WAT depot expansion and lower circulating levels of both triglycerides and free glycerol as compared to control naïve mice (*SI Appendix, Fig. S2 A–C*). Furthermore, post-

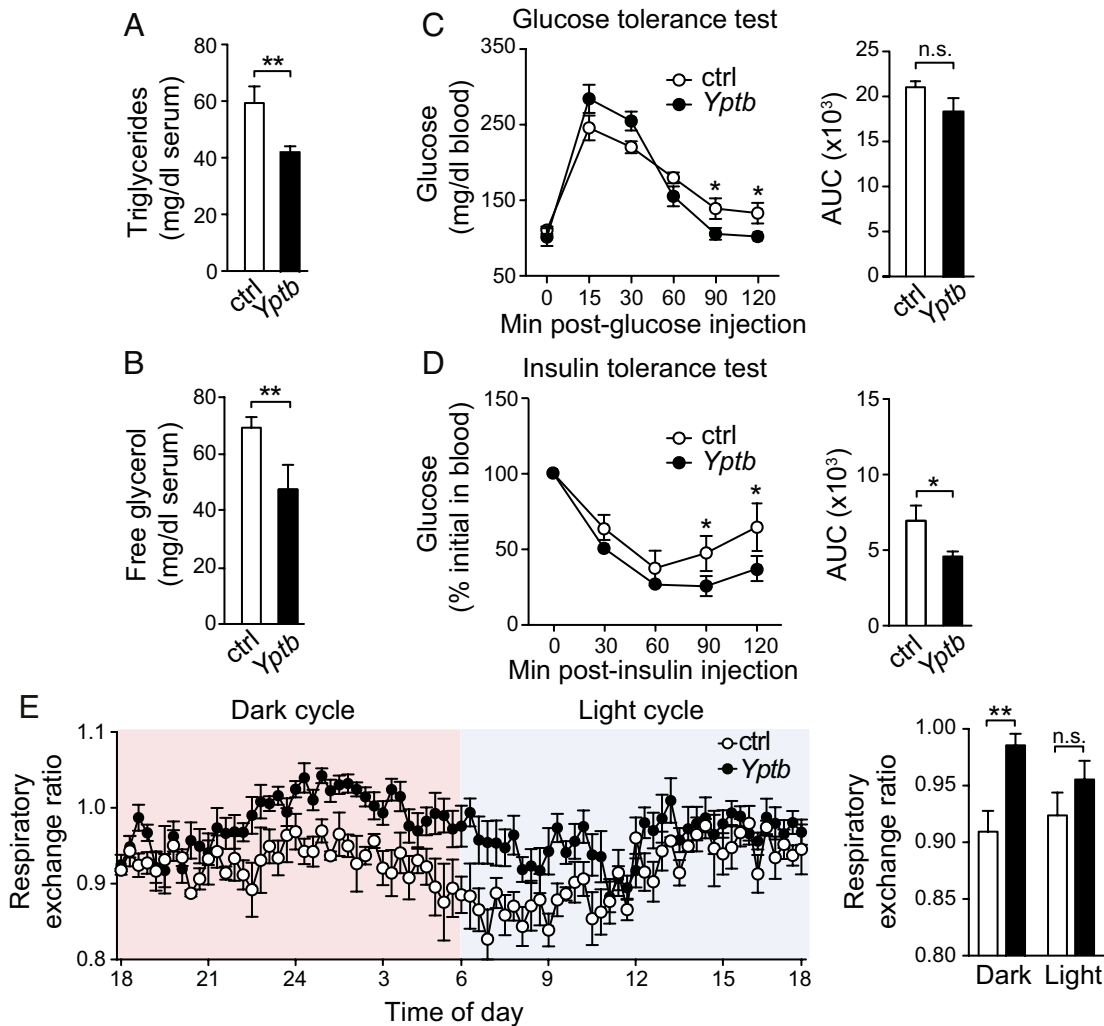


Fig. 2. Prior gut infection can enhance host carbohydrate metabolism. (A–E) Analyses were performed at >15 wk post-*Y. pseudotuberculosis* (*Yptb*) infection. Naïve mice were used as a control (ctrl). (A and B) Triglyceride (A) and free glycerol (B) levels in the serum of fasting mice. (C) Glucose tolerance test results (Left) with area under the curve (AUC, Right). (D) Insulin tolerance test results (Left) with AUC (Right). (E) Respiratory exchange ratio (RER) at 18 min intervals (Left) and average RER during the dark and light cycles (Right). Data represent mean \pm SEM ($n \geq 4$ mice per group). * $P < 0.05$; ** $P < 0.01$; n.s., not significant by two-tailed Student's *t* test or (C and D, Left) two-way ANOVA followed by Bonferroni post hoc test. Unless otherwise indicated, data are representative of at least two experiments.

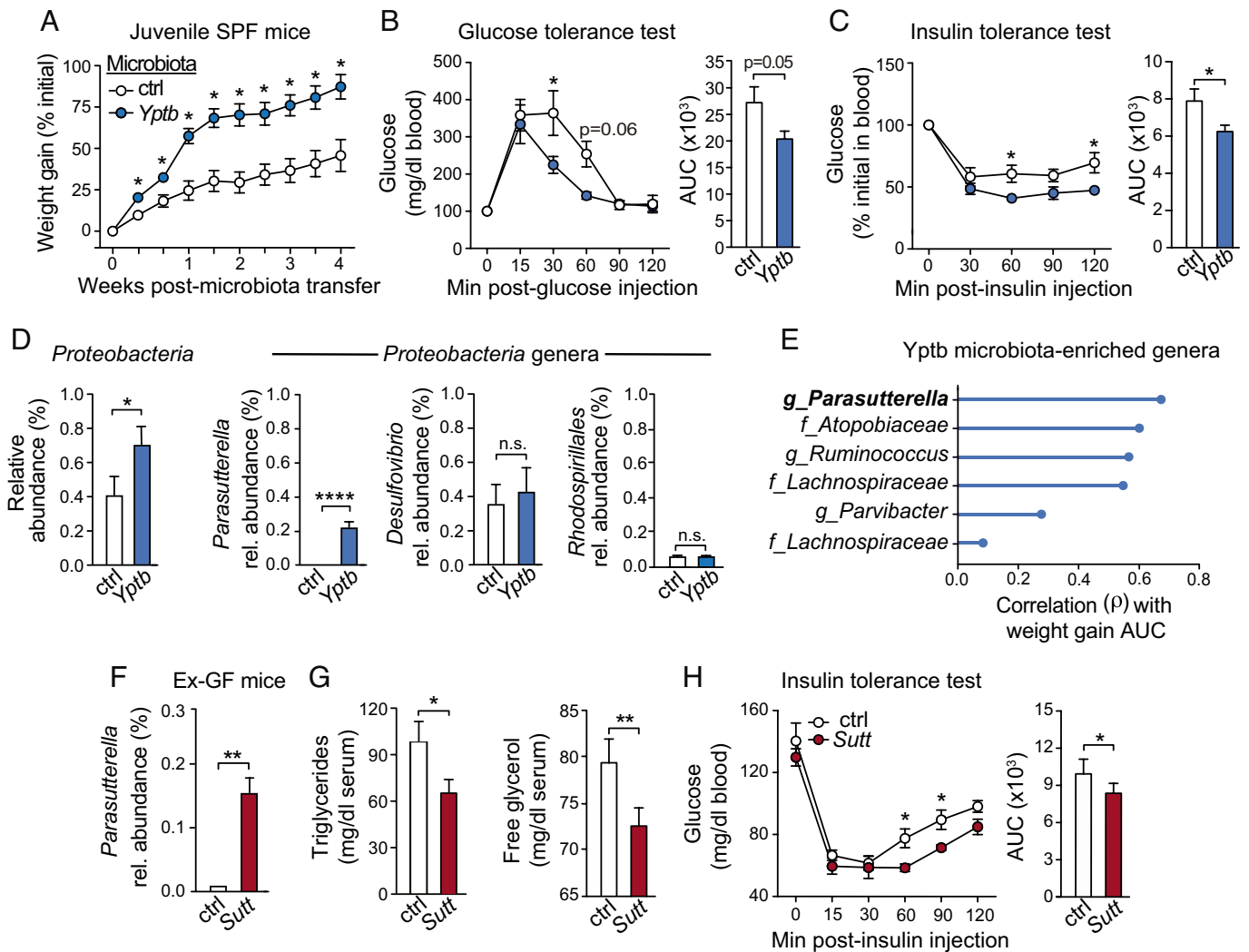


Fig. 3. Infection-elicited microbiota can enhance host carbohydrate metabolism. (A–E) Juvenile specific pathogen-free (SPF) mice were engrafted with microbiota from naïve (control, ctrl) or previously *Y. pseudotuberculosis* (*Yptb*)-infected mice (collected at 17 to 18 wk post-infection). Analyses were performed at >5 wk post-microbiota transfer. Data represent (B and C) one or (A, D, and E) two pooled experiments (n = 4 to 5 or 9 mice per group, respectively). (A) Weight gain (% initial) over time. (B) Glucose tolerance test results (Left) with AUC (Right). (C) Insulin tolerance test results (Left) with AUC (Right). (D) Relative abundance of the *Proteobacteria* phylum (Left) and genera within the *Proteobacteria* (Right). (E) Correlation (Spearman's ρ) of genera abundances with weight gain AUC. Only shown are genera enriched in juvenile SPF mice engrafted with *Yptb* relative to naïve microbiota (\log_2 fold change > 0.5, $P < 0.05$ by two-tailed Mann-Whitney test). Genera are named according to their lowest taxonomic classification (f, family; g, genus). (F–H) Ex-germfree (GF) mice were mono-colonized with *S. wadsworthensis* (*Sutt*) or treated with culture medium as a control (ctrl) prior to housing under SPF conditions. Analyses were performed at 11 wk post-*S. wadsworthensis* colonization. Data represent one experiment (n = 5 mice per group). (F) Relative abundance of the *Parasutterella* genus. (G) Triglyceride (Left) and free glycerol levels (Right) in the serum of fasting mice. (H) Insulin tolerance test results (Left) with AUC (Right). Data represent mean \pm SEM (n \geq 4 mice per group). * $P < 0.05$; ** $P < 0.01$; **** $P < 0.0001$; n.s., not significant by two-tailed Student's *t* test, (B, C, and H, Left) two-way ANOVA followed by Bonferroni post hoc test, or (D and F) two-tailed Mann-Whitney test.

ΔyopM mice outperformed naïve mice in both the GTT and ITT (SI Appendix, Fig. S2 D and E). Thus, gut-restricted pathogens can confer long-term metabolic improvements.

We next sought to explore whether infection-induced metabolic improvement was pathogen-specific. To this end, we used the protozoan parasite *Cryptosporidium tyzzeri*. *C. tyzzeri* is a natural murine pathogen that causes infection similar to water-borne cryptosporidium infection in humans, a leading cause of childhood diarrhea among under-resourced populations (25). Like *Yptb*, *C. tyzzeri* is cleared within 4 wk post-infection (25). Prior *C. tyzzeri* infection triggered pronounced weight gain, WAT depot expansion, and lower circulating levels of triglycerides and free glycerol (SI Appendix, Fig. S3 A–C). Furthermore, post-*C. tyzzeri* mice outperformed naïve mice in both the GTT and ITT (SI Appendix, Fig. S3 D and E). Thus, remodeling of host metabolism can occur in the context of diverse gut infections.

Prior Gut Infection can Remodel Host Metabolism toward Carbohydrate Usage. The improved glucose disposal that we observed in previously *Yptb*, *ΔyopM*, and *C. tyzzeri*-infected mice suggested, among other possibilities, that prior gut infection could shift host metabolism toward the usage of carbohydrates, a major source of glucose. To explore this possibility, we subjected post-*Yptb* mice to indirect calorimetry, a method that can infer energy usage (carbohydrates vs. fat) based on the respiratory exchange ratio (RER), the ratio of carbon dioxide produced to oxygen consumed (26). A higher RER indicates preferential usage of carbohydrates (26), and indeed, the RER of post-*Yptb* mice was higher than that of naïve mice during the dark cycle (at night, when mice are most active). Thus, prior gut infection can remodel host metabolism to preferentially utilize carbohydrates over other macronutrients such as fat (Fig. 2E).

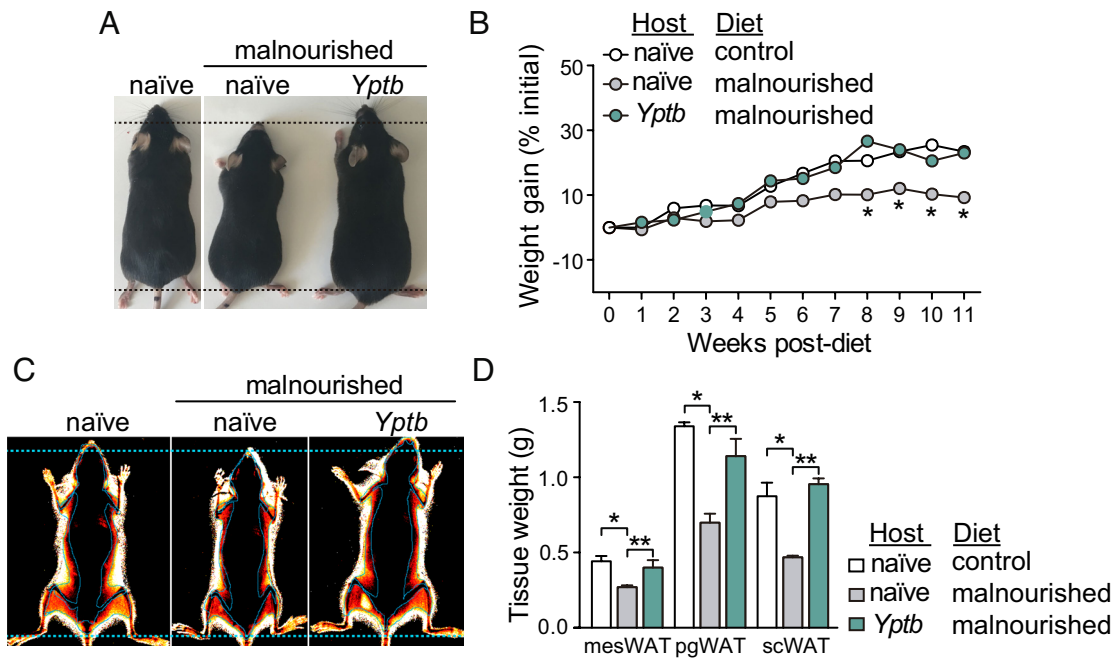


Fig. 4. Infection-induced carbohydrate metabolism can sustain host fitness during nutrient restriction. (A–D) Naïve or previously *Y. pseudotuberculosis* (*Yptb*)-infected mice (at 4 wk post-infection) were placed onto a control or low-protein/fat (malnourished). Analyses were performed at 11 wk post-diet. Data are representative of two experiments. (A) Representative images of malnourished diet-induced stunting. (B) Weight gain (% initial) over time. The *Yptb* control diet group and error bars are not shown for visual clarity. All statistical comparisons were made against the naïve control diet group. The *Yptb* control diet group was not significantly different from the naïve control diet group at any time point. (C) Representative X-ray images of peripheral body fat. (D) Weights of WAT depots (mes, mesenteric; pg, perigonadal; sc, subcutaneous). Data represent mean \pm SEM ($n \geq 4$ mice per group). * $P < 0.05$; ** $P < 0.01$ by two-tailed Student's *t* test.

Infection-Elicited Microbiota can Enhance Host Carbohydrate Metabolism. Previously, we showed that prior *Yptb* infection can remodel the gut microbiota long-term (18). This remodeling, which can persist for >15 wk post-infection, is characterized by a pronounced expansion of *Proteobacteria* (18). Accordingly, we next sought to assess whether *Yptb*-elicited microbiota, such as *Proteobacteria*, contribute to the improvement of host metabolism following infection. To this end, we first transferred gut microbiota from naïve or post-*Yptb* mice into germfree (GF) recipient mice, and after 12 wk, assessed metabolic parameters. Remarkably, post-*Yptb* microbiota was sufficient to impose most of the metabolic alterations observed in post-*Yptb* donor mice, including WAT expansion, decreased circulating triglycerides/glycerol, and increased insulin sensitivity, despite not increasing weight gain (SI Appendix, Fig. S4 A–D).

Because GF mice have been shown to have altered metabolism (10), we next assessed whether post-*Yptb* microbiota could improve host metabolism when transferred into mice with intact microbiota. To promote microbiota engraftment, we transferred microbiota into juvenile (3-wk-old) specific pathogen-free (SPF) mice. At >5 wk post-engraftment, post-*Yptb* microbiota was sufficient to enhance weight gain, glucose disposal, and insulin sensitivity in recipient juvenile SPF mice (Fig. 3 A–C). Together, these results support the idea that remodeling of the gut microbiota following prior infection can be sufficient to improve host metabolism for the long-term.

Infection-Elicited Betaproteobacteria Correlate with Enhanced Host Carbohydrate Metabolism. To identify specific taxa within the post-*Yptb* microbiota that may modulate host metabolism, we performed correlation analyses between taxa abundances and metabolic parameters. In our experiment with GF mice, the most enriched phylum, the *Proteobacteria* (SI Appendix, Fig. S4E and Dataset S1), correlated most strongly with insulin sensitivity (lower area under the curve [AUC] in the insulin tolerance test [ITT]) (two-tailed $P = 0.048$, SI Appendix, Fig. S4F and Dataset S1). Within

the *Proteobacteria*, the only enriched genera were *Parasutterella* (*Betaproteobacteria* class), *Desulfovibrio* (*Deltaproteobacteria* class), and an unclassified genus within the *Rhodospirillales* order (*Alphaproteobacteria* class) (SI Appendix, Fig. S4E and Dataset S1). Of these three genera, *Parasutterella* correlated most strongly with insulin sensitivity, following only two *Clostridia* (two-tailed $P = 0.029$, SI Appendix, Fig. S4G and Dataset S1).

We next repeated these analyses for our experiment with juvenile SPF mice. There, the most enriched phylum was again the *Proteobacteria* (Fig. 3D and Dataset S1), though to a lesser extent (1.8-fold) than in our experiment with GF mice (11-fold). However, within the *Proteobacteria*, the only enriched genus was *Parasutterella* (Fig. 3D), with *Parasutterella* being the most enriched genus (60-fold) among all genera (Dataset S1). Consequently, *Parasutterella* correlated most strongly with weight gain (two-tailed $P = 0.002$, Fig. 3E and Dataset S1) and insulin sensitivity (Spearman's $\rho = -0.52$, Dataset S1). Collectively, these results suggest a prominent role for *Parasutterella* in improving host carbohydrate metabolism.

Betaproteobacteria can Enhance Host Carbohydrate Metabolism.

To assess whether *Parasutterella* is sufficient to improve host carbohydrate metabolism, we colonized mice with a cultivable, human-derived isolate of the closely related betaproteobacterium *Sutterella wadsworthensis* (classifiable as *Parasutterella* based on 16S V4 sequence), after multiple attempts to isolate the murine strain proved unsuccessful. To promote engraftment with the human isolate, we first introduced the isolate into GF mice, where it would not face competition from resident microbiota. Following this, we fully conventionalized these mice via housing under SPF conditions. As expected, this procedure increased the abundance of *S. wadsworthensis* (detected as *Parasutterella*) within the gut microbiota (Fig. 3F and Dataset S1). Colonization of ex-GF mice with *S. wadsworthensis* recapitulated the metabolic improvements observed in post-*Yptb* mice, including decreased circulating triglycerides/glycerol and increased insulin sensitivity,

without promoting gain weight (Fig. 3 *G–H* and *SI Appendix, Fig. S5 A and B*). Likewise, *S. wadsworthensis* colonization of juvenile SPF mice also enhanced glucose disposal and insulin sensitivity (*SI Appendix, Fig. S5 C–E*). Thus, these results support the idea that defined taxa, such as *Parasutterella*, that expand following prior gut infection can directly improve host carbohydrate metabolism.

Infection-induced Carbohydrate Metabolism can Sustain Host Fitness during Nutrient Restriction. Throughout evolution, mammals and their associated microbiota have faced periodic (e.g., seasonal) fluctuations in both infection burden and nutrient availability (27–30). Because of the regular co-occurrence of these and other environmental stressors, the presence of one stressor could serve as a reliable cue for the host to mount preparative defenses against other stressors. Accordingly, infection could signal an impending food shortage, in which some macronutrients (carbohydrates, protein, or fat) become more available than others. In this context, an adaptive host strategy could be to specialize in utilization of the macronutrients that are most consistently available or that require less energy to acquire.

In the wild, many rodent species primarily consume carbohydrate-rich, plant-derived foods (e.g., seeds), though as omnivores, they can also complement their diets with animal-derived foods (e.g., insects) that are richer in protein and fat (27, 28). As such, some rodents may be required to subsist largely on carbohydrates during periods when food is scarce. Because food scarcity has, throughout evolution, often co-occurred with disease outbreaks (31–33), we hypothesized that infection would prompt the host to optimize their metabolism toward the usage of carbohydrates.

To explore this possibility, we utilized a low-protein/fat (high-carbohydrate) diet previously shown to induce a state of malnutrition (34, 35). As previously shown, the low-protein/fat diet stunted the growth, weight gain, body fat, and WAT depots of mice, even when food was provided *ad libitum* (Fig. 4 *A–D*). In contrast, under similar dietary conditions, post-*Yptb* mice remained impervious to signs of malnutrition and developed comparably to naïve mice on the control diet (Fig. 4 *A–D*). Thus, prior infection can promote host fitness in the context of limiting dietary settings in which the main source of nutrients is carbohydrates.

Discussion

The long-term consequences of environmental stressors such as infection on host physiology remain largely unexplored. Here, we show that infection-elicited gut microbiota can remodel host metabolism to preferentially utilize carbohydrates, resulting in heightened glucose disposal, WAT expansion, and weight gain. Furthermore, infection-optimized carbohydrate metabolism could sustain host fitness in the context of limited protein and fat availability, preventing the growth stunting (malnutrition) that otherwise occurs in infection-naïve mice.

Our observations add to a growing body of evidence that environmental stressors are in fact necessary for the full development and optimization of host physiology (18, 36). For example, we previously uncovered that nutrient restriction can enhance the formation of immunological memory and thus resistance to subsequent infection (36), while in the present work, we identify essentially the reverse phenomenon that prior infection can trigger host adaptation to nutrient restriction. This reciprocal regulatory structure (i.e., infection priming for nutrient restriction, and nutrient restriction priming for infection) is likely adaptive and may have arisen as a defense against the frequent co-occurrence of food precarity with infection and other stressors throughout mammalian evolution (31, 33, 37).

In modern human settings, food precarity primarily occurs among under-resourced populations, where the staple foods (e.g., corn, potato, and rice) are often high in carbohydrates (38). Because of this, food precarity can preferentially restrict access to protein and fat. Such skews in nutrient intake, through diets high in carbohydrates but low in protein and fat, potentially contribute to the high rates of malnutrition among under-resourced populations (39). This widespread condition induces a range of developmental defects, such as growth stunting (7), and it often afflicts regions simultaneously burdened with high rates of infectious disease (31). Our finding that infection can promote resistance to malnutrition, particularly malnutrition induced by limited access to protein and fat, raises the intriguing possibility that this phenomenon may help to support human fitness and survival in under-resourced settings.

Though we firmly established a role for the gut microbiota in our observed phenotypes, we presently lack a mechanistic understanding of how infection-elicited microbiota can remodel distal tissues (i.e., WAT) and systemic physiology (i.e., carbohydrate metabolism). We hypothesize a prominent role for microbiota-associated molecular patterns (MAMPs) and/or metabolites, since these molecules are known to mediate much of the microbiota's control over host metabolism, for example by modulating the activity of enteroendocrine cells (40). These specialized gut epithelial cells secrete systemically acting hormones that stimulate production of the glucose-disposing signal insulin (41). Furthermore, enteroendocrine hormones can regulate distal tissues such as WAT (42, 43), potentially leading to WAT expansion and weight gain (43, 44). Supporting a role for microbiota-derived MAMPs/metabolites in modulating the enteroendocrine cell activity of previously infected mice, *Parasutterella*, which we showed are elicited by prior infection and sufficient to enhance glucose homeostasis, have been shown to directly adhere to gut epithelial cells (45) and to localize along the entire length of the gastrointestinal tract, both the large intestine and the upper (46) and lower (45) small intestine (duodenum and ileum). These two sites are, respectively, where two major types of enteroendocrine cells, K and L cells, are primarily found (47). Furthermore, *Parasutterella* produce the MAMP lipopolysaccharide (45) and enhance host production of bile acid metabolites (46), both of which have been shown to modulate enteroendocrine cell activity (48, 49). In ongoing studies, we are exploring how *Parasutterella*-associated MAMPs/metabolites potentially synergize to enhance host metabolism long-term after infection.

Study Limitations. Extrapolation of our results to humans is limited by the fact that our study took place in mice and was highly controlled (used defined pathogens and diets). Further studies of heterogeneous human cohorts are warranted to assess the impact of prior infection and/or other environmental exposures on host metabolic status later in life.

Conclusion

Together, our work highlights the fundamental role of infection in mediating host adaptation to nutrient precarity. By probing the long-term impacts of infection on host metabolism, we discovered that infection-induced gut microbiota optimizes host metabolism toward the usage of carbohydrates. Because carbohydrates are often a more available nutrient source than protein or fat, we speculate that infection-optimized carbohydrate metabolism may be adaptive in under-resourced settings where infection and nutrient precarity often co-occur. In contrast, in settings where carbohydrates are overly accessible (such as with a high-sugar Western diet) or restricted (ketogenic diet), infection-induced carbohydrate metabolism may instead be maladaptive.

Methods

Mice. Adult (6 to 8-wk-old) and juvenile (3-wk-old) SPF female mice were acquired through Taconic Biosciences (C57BL/6NTac) or the University of Campinas Multidisciplinary Center for Biological Research (CEMIB) (C57BL/6JUnib). GF C57BL/6 mice were bred and maintained in the National Institute of Allergy and Infectious Diseases (NIAID) Gnotobiotic Animal Facility. All mice were housed at a maximum of five animals per cage in temperature-controlled rooms under a 12-h light/dark cycle and provided water and chow *ad libitum* (Teklad TD.160179 or Nuvilab CR-1 for SPF mice and NIH 31M for GF mice). All mouse procedures were performed under animal study proposals approved by the NIAID Animal Care and Use Committee (LHIM-2E) or the University of Sao Paulo Ethics Committee for the Use of Animals (49/2016).

Y. pseudotuberculosis. *Y. pseudotuberculosis* strains 32777 and 32777 Δ ypM were revived from freezer stocks on MacConkey agar. Individual colonies were cultured overnight in 2 × YT at 25 °C with shaking. Mice were fasted for at least 12 h prior to gavage with 1×10^7 colony forming units in 200 μ L phosphate buffered saline (PBS).

C. tyzzeri. *C. tyzzeri* was propagated in *Irfng*^{-/-} mice as described (25). Mice were gavaged with 1×10^4 cysts in 100 μ L PBS. Mice were not fasted beforehand.

Food Intake. Food intake was calculated by dividing the daily change in food weight by the number of mice per cage for 5 d.

Peripheral Body Fat. Peripheral body fat was assessed using an In-Vivo MS FX PRO (Bruker) in the University of Sao Paulo Center for Research Facilities and Support (CEFAP-USP) using the following settings: high energy X-ray, 0.8 mm filter; total X-ray, no filter. Body fat, lean, and bone area were quantified using Bruker MI software. Peripheral body fat area (%) was calculated using the following formula: $([\text{fat} + \text{lean} + \text{bone area}] - [\text{lean} + \text{bone area}]) / (\text{fat} + \text{lean} + \text{bone area}) * 100$.

Metabolic Markers. Mice were fasted for 12 h prior to collecting serum for assessing the following markers using commercially available kits: adiponectin (R&D Systems), triglycerides (Pointe Scientific), and free glycerol (Sigma).

Adipose Tissue Histology. WAT depots were fixed overnight in 10% paraformaldehyde, after which they were washed with 70% ethanol, sectioned in paraffin (5 μ m thickness), and stained with hematoxylin and eosin (H&E). Adipocyte cell area was assessed using ImageJ.

Flow Cytometry. Adipocyte progenitors were isolated as previously described (50). Briefly, WAT depots were cut into small pieces, suspended in DMEM + 50 mM HEPES + 0.05 mg/mL Liberase TL (Roche) + 0.25 mg/mL DNase I (Sigma) + 1% BSA (low fatty acid), digested for 25 min at 37 °C with agitation, and passed through 70- μ m filters. The resulting single-cell suspensions were then stained in Hank's Balanced Salt Solution (HBSS) with Invitrogen fixable LIVE/DEAD (Thermo Fisher Scientific), stained in 2% fetal bovine serum (FBS) with fluorochrome-conjugated antibodies for identifying adipocyte progenitors, fixed for 30 min using the Fopx3/Transcription Factor Staining Buffer Set (eBioscience), permeabilized, and stained for at least 1 h with a fluorochrome-conjugated antibody against Ki-67 (clone: SolA15). Stained cells were acquired on a BD LSRFortessa with FACSDiva software and analyzed using FlowJo v10. Adipocyte progenitors were identified as follows: live+, lineage- (CD45- [30-F11], CD31- [MEC13.3]), CD29+ (eBioHMb1-1), CD34+ (RAM34), PDGFR α + (APAS), Sca-1+ (D7), and CD24+ (M1/69).

Glucose and Insulin Tolerance Tests. For glucose tolerance tests, mice were fasted for 12 h prior to challenge with glucose (2 g/kg mouse) via intraperitoneal injection or oral gavage. For insulin tolerance tests, mice were fasted for 4 to 6 h prior to intraperitoneal injection with insulin (0.75 U/kg mouse; Novo Nordisk). Blood glucose levels were assessed by tail vein bleeding using a glucometer (Accu-Chek). AUC were determined using Prism software (GraphPad).

Indirect Calorimetry. RER (the ratio of CO₂ produced to O₂ consumed) was assessed using Oxymax small-animal metabolic cages (Columbus Instruments). Mice were individually housed and acclimated to cages for 24 h prior to calibration and measurement of RER over a 24-h period.

Microbiota Preservation and Transfer. Cecae were harvested from 3 to 4 mice per group, and the contents of the harvested ceca were collected in an anaerobic chamber. Cecal contents were suspended in reduced PBS (0.4 g/mL), pooled, mixed 1:1 with a reduced PBS + 20% glycerol solution, passed through a 70- μ m filter, and preserved at -80 °C as aliquots. Prior to transfer into GF or juvenile mice, microbiota aliquots were thawed, mixed 1:1 with reduced PBS (for final concentration of 0.1 g/mL), and administered via oral (200 μ L) and/or rectal gavage (100 μ L per mouse). Gavages were performed twice with up to 3 d between administrations.

Microbiota Analysis. 16S data were generated and analyzed as previously described (18). Mann-Whitney tests were performed in R using a custom script. Correlation analyses were performed in Excel. The significance of correlations was determined in Prism (GraphPad).

S. wadsworthensis Colonization. *S. wadsworthensis* ATCC 51579 was revived from freezer stocks on YCFAC-B plates (Anaerobe Systems). Colonies were picked into 30 mL cooked meat broth (CMB) with glucose, hemin, and vitamin K (Thermo) + 3% formate + 3% fumarate (CMBFF) and cultured overnight at 37 °C in an anaerobic chamber. After centrifugation at 2,500 × g for 10 min, cultures were resuspended in 2 mL fresh CMBFF, and 200 μ L was gavaged per GF mouse immediately after housing under SPF conditions. Sterile CMBFF was used as a control. Additional gavages were performed every other day for 1 wk (four total gavages). When colonizing juvenile SPF mice, mice were fasted for several hours (from the morning until the afternoon) prior to the first two of four total gavages.

Diet Studies. To induce malnutrition, mice were placed onto a diet (Teklad TD.160180) with low levels of protein and fat (7% and 5% w/w, respectively). Control mice were placed onto an isocaloric diet (Teklad TD.160179) with standard levels of protein and fat (20% and 15% w/w, respectively).

Data, Materials, and Software Availability. 16S data were deposited into the Sequence Read Archive (PRJNA819152) (51).

ACKNOWLEDGMENTS. This work was supported by the NIAID Intramural Research Program (ZIAAI001115 and ZIA-AI001132 to Y.B.), the Sao Paulo Research Foundation (FAPESP) (2015/25364-0, 2016/08385-7, and 2021/06881-5 to D.M.d.F.; 2017/02298-8 and 2018/14562-4 to M.K.D.S.; 2018/00458-0 to J.M.S.; 2017/14209-0 to M.D.-F.; 2018/15981-0 to L.M.-S.), Coordination for the Improvement of Higher Education Personnel/National Council for Scientific and Technological Development (CAPES/CNPq) (D.M.d.F.), the Pew Latin American Fellows Program (V.A.-O.), the NIGMS Postdoctoral Research Associate Training (PRAT) Program (FI2GM128736 to A.S.), NIDCR (K99DE31372 to A.S.), and the Helen Hay Whitney Foundation (A.G.Z.). We thank Dr. Boris Striepen (University of Pennsylvania) for providing *Cryptosporidium tyzzeri*. Dana Trageser-Cesler and Cesar Acevedo (NIAID Gnotobiotic Animal Facility), Eliane Mello Gomes for technical assistance, the University of Sao Paulo Center for Research Facilities and Support (CEFAP-USP) staff, the NIAID animal facility staff, and the NIAID Microbiome Program staff.

Author affiliations: ^aDepartment of Immunology, Institute of Biomedical Sciences, University of Sao Paulo, Sao Paulo, SP 05508-000, Brazil; ^bMetaorganism Immunity Section, Laboratory of Host Immunity and Microbiome, National Institute of Allergy and Infectious Diseases, NIH, Bethesda, MD 20892; ^cNational Institute of Allergy and Infectious Diseases Microbiome Program, National Institute of Allergy and Infectious Diseases, NIH, Bethesda, MD 20892; and ^dDepartment of Clinical and Toxicological Analysis, Faculty of Pharmaceutical Sciences, University of Sao Paulo, Sao Paulo, SP 05508-000, Brazil

Author contributions: M.K.D.S., V.A.-O., A.S., D.M.d.F., and Y.B. designed research; M.K.D.S., V.A.-O., A.S., J.P.T.G., R.W.A.-C., S.-J.H., A.G.Z., T.W.H., and D.M.d.F. performed research; A.C., J.M.S., M.D.-F., L.M.-S., W.M.T., N.O.S.C., M.R., and S.J. contributed new reagents/analytic tools; M.K.D.S., V.A.-O., A.S., D.M.d.F., and Y.B. analyzed data; and M.K.D.S., V.A.-O., A.S., D.M.d.F., and Y.B. wrote the paper.

Reviewers: W.S.G., Harvard T.H. Chan School of Public Health; and M.R., University of California San Diego.

The authors declare no competing interest.

Copyright © 2023 the Author(s). Published by PNAS. This open access article is distributed under [Creative Commons Attribution-NonCommercial-NoDerivatives License 4.0 \(CC BY-NC-ND\)](https://creativecommons.org/licenses/by-nc-nd/4.0/).

¹Present Address: Department of Integrative Biology and Physiology, University of California, Los Angeles, CA 90095.

1. C. R. Voolstra, M. Ziegler, Adapting with microbial help: Microbiome flexibility facilitates rapid responses to environmental change. *BioEssays* **42**, e2000004 (2020).
2. K. Troha, J. S. Ayres, Metabolic adaptations to infections at the organismal level. *Trends Immunol.* **41**, 113–125 (2020).
3. N. Collins, Y. Belkaid, Control of immunity via nutritional interventions. *Immunity* **55**, 210–223 (2022).
4. E. Ansaldi, T. K. Farley, Y. Belkaid, Control of immunity by the microbiota. *Annu. Rev. Immunol.* **39**, 449–479 (2021).
5. K. R. Amato, Incorporating the gut microbiota into models of human and non-human primate ecology and evolution. *Am. J. Phys. Anthropol.* **159**, S196–215 (2016).
6. P. J. Turnbaugh *et al.*, The effect of diet on the human gut microbiome: A metagenomic analysis in humanized gnotobiotic mice. *Sci. Transl. Med.* **1**, 6ra14 (2009).
7. L. V. Blanton, Gut bacteria that prevent growth impairments transmitted by microbiota from malnourished children. *Science* **351**, aad3311 (2016), 10.1126/science.aad3311.
8. D. Festi *et al.*, Gut microbiota and metabolic syndrome. *World J. Gastroenterol.* **20**, 16079–16094 (2014).
9. F. Bäckhed, J. K. Manchester, C. F. Semenkovich, J. I. Gordon, Mechanisms underlying the resistance to diet-induced obesity in germ-free mice. *Proc. Natl. Acad. Sci. U.S.A.* **104**, 979–984 (2007).
10. F. Bäckhed *et al.*, The gut microbiota as an environmental factor that regulates fat storage. *Proc. Natl. Acad. Sci. U.S.A.* **101**, 15718–15723 (2004).
11. H. Plovier *et al.*, A purified membrane protein from *Akkermansia muciniphila* or the pasteurized bacterium improves metabolism in obese and diabetic mice. *Nat. Med.* **23**, 107–113 (2017).
12. S. Devkota *et al.*, Dietary-fat-induced taurocholic acid promotes pathobiont expansion and colitis in *IL10^{-/-}* mice. *Nature* **487**, 104–108 (2012).
13. J. M. Natividad *et al.*, *Bilophila wadsworthia* aggravates high fat diet induced metabolic dysfunctions in mice. *Nat. Commun.* **9**, 2802 (2018).
14. J. L. Sonnenburg, E. D. Sonnenburg, Vulnerability of the industrialized microbiota. *Science* **366** (2019).
15. D. Ramanan *et al.*, Helminth infection promotes colonization resistance via type 2 immunity. *Science* **352**, 608–612 (2016).
16. S. P. Rosshart *et al.*, Wild mouse gut microbiota promotes host fitness and improves disease resistance. *Cell* **171**, 1015–1028.e1013 (2017).
17. B. Hild *et al.*, Neonatal exposure to a wild-derived microbiome protects mice against diet-induced obesity. *Nat. Metab.* **3**, 1042–1057 (2021).
18. A. Stacy *et al.*, Infection trains the host for microbiota-enhanced resistance to pathogens. *Cell* **184**, 615–627.e617 (2021).
19. C. A. Thaiss *et al.*, Hyperglycemia drives intestinal barrier dysfunction and risk for enteric infection. *Science* **359**, 1376–1383 (2018).
20. K. K. Sanchez *et al.*, Cooperative metabolic adaptations in the host can favor asymptomatic infection and select for attenuated virulence in an enteric pathogen. *Cell* **175**, 146–158.e115 (2018).
21. D. M. Fonseca *et al.*, Microbiota-dependent sequelae of acute infection compromise tissue-specific immunity. *Cell* **163**, 354–366 (2015).
22. L. Vishvanath, R. K. Gupta, Contribution of adipogenesis to healthy adipose tissue expansion in obesity. *J. Clin. Invest.* **129**, 4022–4031 (2019).
23. S. Virtue, A. Vidal-Puig, GTTs and ITTs in mice: Simple tests, complex answers. *Nat. Metab.* **3**, 883–886 (2021).
24. S. J. Han *et al.*, White adipose tissue is a reservoir for memory T cells and promotes protective memory responses to infection. *Immunity* **47**, 1154–1168.e1156 (2017).
25. A. Sateriale *et al.*, A genetically tractable, natural mouse model of cryptosporidiosis offers insights into host protective immunity. *Cell Host. Microbe*. **26**, 135–146.e135 (2019).
26. J. Rozman, M. Klingenspor, M. Hrabě de Angelis, A review of standardized metabolic phenotyping of animal models. *Mamm. Genome*. **25**, 497–507 (2014).
27. O. J. Reichman, Relation of desert rodent diets to available resources. *J. Mammal.* **56**, 731–751 (1975).
28. C. H. S. Watts, R. W. Braithwaite, The diet of *Rattus lutreolus* and five other rodents in Southern Victoria. *Wildlife Res.* **5**, 47–57 (1978).
29. A. Bajzer *et al.*, Medium-term temporal stability of the helminth component community structure in bank voles (*Clethrionomys glareolus*) from the Mazury Lake District region of Poland. *Parasitology* **130**, 213–228 (2005).
30. C. Kiffner, T. Vor, P. Hagedorn, M. Niedrig, F. Rühle, Factors affecting patterns of tick parasitism on forest rodents in tick-borne encephalitis risk areas, Germany. *Parasitol. Res.* **108**, 323–335 (2011).
31. J. L. Watson, J. A. Berkley, The impact of malnutrition on childhood infections. *Curr. Opin. Infect. Dis.* **31**, 231–236 (2018).
32. A. Gwela, E. Mupere, J. A. Berkley, C. Lancioni, Undernutrition, host immunity and vulnerability to infection among young children. *Pediatr. Infect. Dis. J.* **38**, e175–e177 (2019).
33. E. Mertens, J. L. Peñalvo, The burden of malnutrition and fatal COVID-19: A global burden of disease analysis. *Front. Nutr.* **7**, 619850 (2021).
34. E. M. Brown *et al.*, Diet and specific microbial exposure trigger features of environmental enteropathy in a novel murine model. *Nat. Commun.* **6**, 7806 (2015).
35. N. R. Teodósio, E. S. Lago, S. A. Romani, R. C. Guedes, A regional basic diet from northeast Brazil as a dietary model of experimental malnutrition. *Arch. Latinoam. Nutr.* **40**, 533–547 (1990).
36. N. Collins *et al.*, The bone marrow protects and optimizes immunological memory during dietary restriction. *Cell* **178**, 1088–1101.e1015 (2019).
37. P. C. Calder, A. A. Jackson, Undernutrition, infection and immune function. *Nutr. Res. Rev.* **13**, 3–29 (2000).
38. S. Ruan *et al.*, Staple food and health: A comparative study of physiology and gut microbiota of mice fed with potato and traditional staple foods (corn, wheat and rice). *Food & Function* **12**, 1232–1240 (2021).
39. Z. A. Bhutta *et al.*, Severe childhood malnutrition. *Nat. Rev. Dis. Primers* **3**, 17067 (2017).
40. Y. Fan, O. Pedersen, Gut microbiota in human metabolic health and disease. *Nat. Rev. Microbiol.* **19**, 55–71 (2021).
41. F. Preitner *et al.*, Gluco-incretins control insulin secretion at multiple levels as revealed in mice lacking GLP-1 and GIP receptors. *J. Clin. Invest.* **113**, 635–645 (2004).
42. H. Hauner, G. Glatting, D. Kaminska, E. F. Pfeiffer, Effects of gastric inhibitory polypeptide on glucose and lipid metabolism of isolated rat adipocytes. *Ann. Nutr. Metab.* **32**, 282–288 (1988).
43. L. Getty-Kaushik, D. H. Song, M. O. Boylan, B. E. Corkey, M. M. Wolfe, Glucose-dependent insulinotropic polypeptide modulates adipocyte lipolysis and reesterification. *Obesity (Silver Spring)* **14**, 1124–1131 (2006).
44. R. Ugleholdt *et al.*, Transgenic rescue of adipocyte glucose-dependent insulinotropic polypeptide receptor expression restores high fat diet-induced body weight gain. *J. Biol. Chem.* **286**, 44632–44645 (2011).
45. K. Hiippala, V. Kainulainen, M. Kalliomäki, P. Arkkila, R. Satokari, Mucosal prevalence and interactions with the epithelium indicate commensalism of *Sutterella* spp. *Front. Microbiol.* **7**, 1706 (2016).
46. T. Ju, J. Y. Kong, P. Stothard, B. P. Willing, Defining the role of *Parasutterella*, a previously uncharacterized member of the core gut microbiota. *ISME J.* **13**, 1520–1534 (2019).
47. R. Gutierrez-Aguilar, S. C. Woods, Nutrition and L and K-enteroendocrine cells. *Curr. Opin. Endocrinol. Diabetes Obes.* **18**, 35–41 (2011).
48. L. J. Lebrun *et al.*, Enteroendocrine L cells sense LPS after gut barrier injury to enhance GLP-1 secretion. *Cell Rep.* **21**, 1160–1168 (2017).
49. S. Katsuma, A. Hirasawa, G. Tsujimoto, Bile acids promote glucagon-like peptide-1 secretion through TGR5 in a murine enteroendocrine cell line STC-1. *Biochem. Biophys. Res. Commun.* **329**, 386–390 (2005).
50. C. D. Church, R. Berry, M. S. Rodeheffer, Isolation and study of adipocyte precursors. *Methods Enzymol.* **537**, 31–46 (2014).
51. M. K. De Siqueira *et al.*, Infection-induced microbiota enhances host adaptation to nutrient restriction. *Sequence Read Archive*. <https://www.ncbi.nlm.nih.gov/bioproject/PRJNA819152/>. Deposited 23 March 2022.